

Article

Not peer-reviewed version

Hybrid FSO/RF Communications in Space–Air–Ground Integrated Networks: A Reduced Overhead Link Selection Policy

[Petros S. Bithas](#)^{*}, [Hector E. Nistazakis](#), Athanassios Katsis, [Liang Yang](#)

Posted Date: 11 January 2024

doi: 10.20944/preprints202401.0821.v1

Keywords: Composite fading; free space optical communications; hybrid FSO/RF communications; link selection; space-air-ground integrated networks




Preprints.org is a free multidiscipline platform providing preprint service that is dedicated to making early versions of research outputs permanently available and citable. Preprints posted at Preprints.org appear in Web of Science, Crossref, Google Scholar, Scilit, Europe PMC.

Copyright: This is an open access article distributed under the Creative Commons Attribution License which permits unrestricted use, distribution, and reproduction in any medium, provided the original work is properly cited.

Article

Hybrid FSO/RF Communications in Space–Air–Ground Integrated Networks: A Reduced Overhead Link Selection Policy

Petros S. Bithas^{1,*} , Hector E. Nistazakis², Athanassios Katsis³, and Liang Yang⁴

¹ Department of Digital Industry Technologies, National and Kapodistrian University of Athens (NKUA), Psahna, 34400, Evia, Greece; pbithas@dind.uoa.gr

² Department of Physics, National and Kapodistrian University of Athens, 15784, Athens, Greece; enistaz@phys.uoa.gr

³ Department of Social and Educational Policy, University of the Peloponnese, 20100 Korinthos, Greece; katsis@uop.gr

⁴ College of Computer Science and Electronic Engineering, Hunan University, Changsha 410082, China; liangy@hnu.edu.cn

* Correspondence: pbithas@dind.uoa.gr

Abstract: Space–air–ground integrated network (SAGIN) is considered as an enabler for the sixth-generation (6G) networks. By integrating terrestrial and non-terrestrial (satellite, aerial) networks, SAGIN seem to be a quite promising solution to provide reliable connectivity everywhere and all the time. Their availability can be further enhanced if hybrid free space optical (FSO)/radio frequency (RF) links are adopted. In this paper, the performance of a hybrid FSO/RF communication system operating in SAGIN has been analytically evaluated. In the considered system, a high altitude platform station (HAPS) is used to forward the satellite signal to the ground station. Moreover, the FSO channel model assumed takes into account the turbulence, pointing errors and path losses, while for the RF links, a relatively new composite fading model has been considered. In this context, a new link selection scheme has been proposed that is designed to reduced the signaling overhead required for the switching operations between the RF and FSO links. The analytical framework that has been developed is based on the Markov chain theory. Capitalizing on this framework, the performance of the system has been investigated using the criteria of outage probability and the average number of link estimations. The numerical results presented reveal that the new selection scheme offers a good compromise between performance and complexity.

Keywords: composite fading; free space optical communications; hybrid FSO/RF communications; link selection; space-air-ground integrated networks

1. Introduction

In recent years, the concept of space-air-ground integrated network (SAGIN), which integrates satellite, aerial, and terrestrial communications, has emerged as a noteworthy architectural paradigm [1]. This integrated approach has received significant research attention, in an evolving and compelling area of study as is the sixth generation (6G) communication network [2]. SAGIN aim to address the connectivity challenges that arise in remote and hard-to-reach areas by offering a cost-effective and high-capacity solution. Therefore, this type of networks seems to be the only path towards realizing the Internet of remote things. However, despite the undoubtedly benefits of these networks, they also come with certain disadvantages, including unbalanced distribution of resources [3], channel impairments [4], complexity and integration challenges [5], security concerns [2]. SAGIN can overcome some of the limitations associated with traditional communication methods by incorporating free space optical (FSO) links. FSO-assisted SAGIN will lead to improved performance, reliability, and adaptability in diverse operational scenarios, since they will offer increased bandwidth availability, low latency, increased security, and immunity to electromagnetic interference [6].

However, FSO communication are also prone to various environmental and channel attenuation effects, e.g., atmospheric turbulence, that result to severe degradation of the performance, e.g., [7,8]. An alternative approach to mitigating the impact of atmospheric turbulence involves integrating radio-frequency (RF) links alongside the FSO ones to exploit their complementary attributes. This hybrid RF/FSO communication strategy allows for the advantages of both RF and FSO technologies, and as a result effectively minimizing the detrimental effects associated with adverse weather conditions [9]. The performance of these systems can be further enhanced if unmanned aerial vehicles (UAVs) or high altitude platforms station (HAPS) are used as relays [10,11]. The cooperation of HAPS and low Earth orbit (LEO) satellites is expected to guarantee higher capacity with lower propagation delay.

1.1. Relevant Works

In the past few years, there have been numerous contributions within the realm of integrated networks that combine FSO and RF technologies with satellite and aerial components, e.g., [12–18]. In [12], an analytical expression for the outage probability (OP) in a SAGIN has been presented, taking into account the impact of pointing errors in the satellite-aerial segment. In [13], based on the selective decode-and-forward (DF) protocol the ergodic capacity of a multiuser downlink SAGIN has been analytically studied. In [14], the assessment of a dual-hop hybrid FSO/RF SAGIN has been analytically investigated using the criteria of OP and bit error probability. In [15] a HAPS-selection scheme has been introduced in a cooperative SAGIN communication scenario. This scheme was based on a signal-to-noise ratio (SNR) criterion, while the OP analysis that was presented took also into account various impairment effects, including atmospheric turbulence and pointing errors.

In [16], the utilization of a LEO satellite was explored in order to enhance the performance of two mixed FSO/RF HAPS-assisted communication systems. Moreover, [17] focuses on a hybrid FSO/RF and SAGIN, in which the OP and the average symbol error probability were investigated, taking also into account various propagation phenomena such as turbulence and weather effects. Finally, in [18], the performance of hybrid FSO/RF relay systems in satellite terrestrial integrated network was investigated, in which the effect of weather conditions was also taken into consideration. In that study, three different schemes were designed on HAPS, while reconfigurable intelligent surface (RIS) assisted UAVs were also considered. It is noted that in most of the aforementioned studies, valuable insights were also provided that were based on the asymptotic expressions that have been also provided. Moreover, another parameter that is very important for the performance of hybrid RF/FSO SAGIN is signalling overhead. In particular, for the various network operations that frequently take place in these systems, e.g., handover, link switching, signaling exchanges between the network nodes should be made. However, this signaling is responsible for latency increase and effective capacity reduction. Therefore, algorithms that will efficiently achieve the trade-off between signaling overhead and system's performance should be proposed [19,20].

1.2. Contributions

Motivated by this, in this paper, we introduce a lower signaling overhead channel selection scheme in hybrid FSO/RF SAGIN. More specifically, the contributions of this paper are summarized as follows:

- A new channel selection scheme has been proposed and used in a hybrid FSO/RF SAGIN dual-hop communication scenario. The new scheme is designed to offer reduced overhead signalling with satisfactory performance.
- For the new scheme, based on the Markov chain theory, exact analytical expressions are derived for the statistics of the end-to-end output SNR. The analysis presented takes also into account the impact of atmospheric turbulence and pointing errors (for the FSO link) as well as multipath fading and shadowing (for the RF link).

- In the high SNR regime, simpler asymptotic closed-form expressions are also provided, which have been employed to elaborate on the physical insights of the considered scenarios.
- The analytical results derived are used to study the OP of the proposed scheme, while the signaling overhead has been also quantified using the criteria of average number of links estimation (NLE) and switching probability (SP).
- The numerical evaluated results that are presented, reveal the reduction of the computational complexity, which results to important energy savings, without a significantly affecting the performance.

The remainder of this paper is as follows. In Section 2, the system and channel models under investigation are presented. In Section 3, a Markov chain based analytical framework is proposed that is used to investigate the end-to-end OP. In Section 4, various numerically evaluated results are presented and discussed, while in Section 5, the conclusions can be found.

2. System and Channel Models

2.1. System Model

We consider a dual-hop SAGIN where the LEO satellite (S) communicates with the ground station (G), with the aid of a HAPS (H), as it is shown in Figure 1. The direct S-G link is assumed to be blocked due to severe shadowing and atmospheric attenuation phenomena. In the first phase of communication, S transmits the signal to H using an FSO link. In that case, the received SNR at the HAPS is given by¹

$$\gamma_1 = \frac{(\eta P_f G_{Tf} G_{Rf} I)^b}{F^b \sigma_f^2}, \quad (1)$$

where η denotes the optical-to-electrical conversion coefficient, P_f denotes the transmit power of the FSO communication system, G_{Tf}, G_{Rf} are the transmit and receive telescope gains, respectively, I denotes the random fluctuations of the received amplitude, $F = (4\pi d_k / \lambda_f)$, where λ_f is the wavelength of the FSO communications, and d_k denotes the transmission distance between the FSO transmitter and FSO receiver (with $k \in s, h$) as it is also shown in Figure 1. Moreover, $b = 1$ and $b = 2$ for heterodyne and direct detection schemes, respectively, while σ_f^2 denotes the noise variance of the additive white Gaussian noise (AWGN).

As far as the RF communication links are concerned, the instantaneous received SNR per symbol at the G is given by

$$\gamma_2 = \bar{\gamma}_2 |h_r|^2, \quad (2)$$

where $\bar{\gamma}_2$ is defined as

$$\bar{\gamma}_2 = \frac{P_t}{N_0} \left(\frac{G_{Tr} G_{Rr} \lambda_r^2}{16\pi^2 d_h^v} \right). \quad (3)$$

In (3), G_{Tr}, G_{Rr} denote the transmit and receive antenna gains for the RF systems, respectively, λ_r is the RF wavelength, and d_h denotes the H-G distance. Moreover, $|h_r|$ denotes the normalized magnitude of the channel fading coefficient, $|\cdot|$ denotes absolute value.

The H acts as a relay and implements DF protocol. Therefore, if H has correctly decoded the received from the satellite signal, it forwards it to the G using hybrid RF/FSO communications. At the G, a new link selection policy is adopted that offers reduced overhead in terms of channel monitoring. According to this policy, it is examined whether the previously selected link exceeds a predefined switching threshold γ_{th} . If this is the case, the algorithm remains to that link, otherwise it switches to

¹ Without losing the generality, it is assumed that at the received SNR, subscript 1 denotes FSO links and subscript 2 denotes RF links.

the link (after examining both RF and FSO ones) that has the highest SNR value. Based on the above definitions, the end-to-end received instantaneous SNR at the G is given by

$$\gamma_o = \min\{\gamma_1, \gamma_t\} \quad (4)$$

where γ_t denotes the instantaneous received SNR at the G for the H-G link as a result of the mode of operation of the proposed policy. Next, the channel models assumed for both communication links are presented.

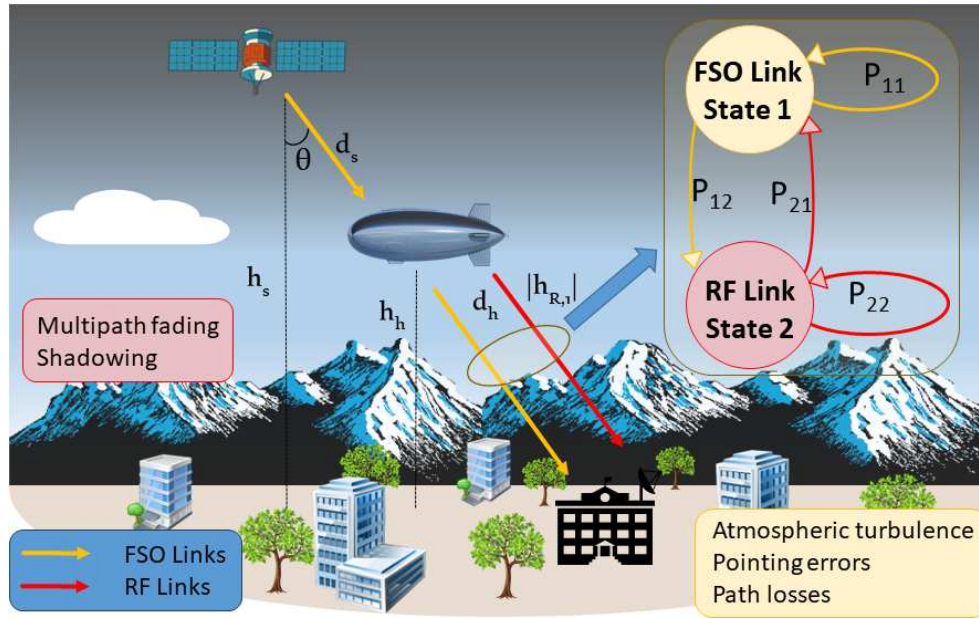


Figure 1. System Model.

2.2. Channel Model

For the FSO links, the joined impact of atmospheric turbulence-induced fading (modeled using the gamma-gamma distribution [21]), pointing errors (modeled using the Rayleigh distribution [22]), and path loss (based on the Beers-Lampert law [23]) have been taken into account. In that case, it can be proved that the cumulative distribution function (CDF) of the received SNR is given by [14]

$$F_{\gamma_1}(\gamma) = \mathcal{A} G_{b+1, 3b+1}^{3b, 1} \left(\frac{D^b \gamma}{b^2 \bar{\gamma}_1^f} \middle| \begin{matrix} 1, \Delta_{b, \zeta^2+1} \\ \Delta_{b, \zeta^2}, \Delta_{b, \alpha}, \Delta_{b, \beta}, 0 \end{matrix} \right), \quad (5)$$

where $D = \alpha\beta\kappa$, $\mathcal{A} = \frac{\zeta^2 b^{\alpha+\beta-2}}{(2\pi)^{b-1} \Gamma(\alpha) \Gamma(\beta)}$, $\Delta_{x,y} = \frac{y}{x}, \frac{y+1}{x}, \frac{y+x-1}{x}$, while $\bar{\gamma}_1^f$ denotes the average received SNR defined as

$$\bar{\gamma}_1 = \frac{\eta P_f G_{Tf} G_{Rf} \kappa I_p^f A_0}{F_f^b \sigma_f^2}, \quad (6)$$

with $\kappa = \frac{\zeta^2}{\zeta^2+1}$. Moreover, I_p^f denotes the path loss attenuation, A_0 is the fraction of total power collected at the receiver aperture, F_f is the free space loss defined as $F_f = \frac{4\pi d_k}{\lambda_f}$. Moreover, ζ denotes the pointing error parameter coefficient, while α and β are large and small scale turbulence parameters, respectively, related to the scattering environment, whose expressions are provided next. Finally,

$G_{p,q}^{m,n}[\cdot|\cdot]$ denotes the Meijer's G-function [24, eq. (9.301)], and $\Gamma(\cdot)$ the gamma function [24, eq. (8.310/1)]. The corresponding PDF expression is given by

$$f_{\gamma_1}(\gamma) = \frac{\mathcal{B}}{\gamma} G_{1,3}^{3,0} \left(D \left(\frac{\gamma}{\tilde{\gamma}_1^f} \right)^{1/b} \middle| \begin{matrix} \zeta^2+1 \\ \zeta^2, \alpha, \beta \end{matrix} \right), \quad (7)$$

where $\mathcal{B} = \frac{\zeta^2}{b\Gamma(\alpha)\Gamma(\beta)}$. As far as the large and small scale turbulence parameters are concerned, they are, respectively, defined as [21]

$$\alpha = \left\{ 5.95(h_k - h_\ell)^2 \sec(\theta)^2 \left(\frac{2W_0}{r} \right)^{5/3} \left(\frac{\Delta_{pe}}{W} \right)^2 + \left[\exp \left(\frac{0.49\sigma^2}{(1 + 0.56\sigma^{12/5})^{7/6}} \right) - 1 \right] \right\}^{-1}, \quad (8)$$

$$\beta = \left[\exp \left(\frac{0.51\sigma^2}{(1 + 0.69\sigma^{12/5})^{5/6}} \right) - 1 \right]^{-1}, \quad (9)$$

where the pair k, ℓ takes values s, h when S-H link is considered and h, p , when H-G link is considered. Next, details for the parameters included in (8) and (9) will be provided. More specifically, in (8), σ^2 denotes the Rytov variance and is given by

$$\sigma^2 = 2.25k_1^{7/6} (h_k - h_\ell)^{5/6} \sec(\theta)^{11/6} \times \int_{h_\ell}^{h_k} C_n^2(h) \left(1 - \frac{h - h_\ell}{h_k - h_\ell} \right)^{5/6} \left(\frac{h - h_\ell}{h_k - h_\ell} \right)^{5/6} dh. \quad (10)$$

Moreover, $C_n^2(h)$ denotes the refractive index structure parameter, which is defined as [25]

$$C_n^2(h) = 0.00594 \left(\frac{w}{27} \right)^2 (10^{-5}h)^{10} \exp \left(-\frac{h}{1000} \right) + 2.7 \cdot 10^{-16} \exp \left(-\frac{h}{1500} \right) + C_n^2(0) \exp \left(-\frac{h}{100} \right), \quad (11)$$

where $C_n^2(0) = 1.7 \times 10^{-14} m^{-2/3}$ and w denotes the wind velocity. Moreover, in (8), W_0 denote the beam size at the transmitter, while the corresponding parameter at the receiver is given by $W = W_0 \sqrt{\Theta^2 + \Lambda^2}$, where $\Theta = 1 - \frac{d_k}{F_0}$ and $\Lambda = \frac{2d_k}{k_1 W_0^2}$. Furthermore, F_0 denotes the phase front radius of the curvature of the beam at the transmitter and $d_k = \frac{h_k}{\cos(\theta)}$. Additionally, the Fried parameter r is given by

$$r = \left[0.42 \sec(\theta) k_1^2 \int_{h_\ell}^{h_k} C_n^2(h) dh \right]^{-3/5}, \quad (12)$$

while $\Delta_{pe} = \frac{\sigma_{pe}^2}{d_k^2}$ denotes the beam-wander-induced pointing errors, with the beam-wander-induced pointing error variance given by

$$\sigma_{pe}^2 = 0.54 (h_k - h_\ell)^2 \sec(\theta)^2 \left(\frac{\lambda_f}{2W_0} \right)^2 \times \left(\frac{2W_0}{r} \right)^{5/3} \left[1 - \left(\frac{C_r^2 W_0^2 / r^2}{1 + C_r^2 W_0^2 / r^2} \right)^{1/6} \right], \quad (13)$$

with $C_r = 2\pi$ being the scaling constant.

For the RF links, the PDF of the instantaneous received SNR at the G can be expressed as [26, eq. (7)]

$$f_{\gamma_2}(\gamma) = \gamma^{-1} \mathcal{S}_1 G_{2,2}^{2,2} \left(\frac{m_1 m_2 \gamma}{\bar{\gamma}_2} \middle| \begin{matrix} 1-\alpha_2, 1-\alpha_1 \\ m_1, m_2 \end{matrix} \right), \quad (14)$$

where $\mathcal{S}_1 = \frac{1}{\Gamma(m_1)\Gamma(m_2)\Gamma(\alpha_1)\Gamma(\alpha_2)}$. It is noted that (14) is a experimentally verified composite fading model that accurately describes both small scale and large scale fading effects in UAV-to-ground communication scenarios. In particular coefficients m_1, m_2 the severity of the small scale fading, i.e., as m_1, m_2 increase line-of-sight conditions are approximated. Moreover, coefficients α_1, α_2 are related to the secerity of the shadowing, i.e., lower values of α_1, α_2 result to lighter shadowing conditions. The corresponding CDF expression is given by

$$F_{\gamma_2}(\gamma) = \mathcal{S}_1 G_{3,3}^{2,3} \left(\frac{m_1 m_2 \gamma}{\bar{\gamma}_2} \middle| \begin{matrix} 1-\alpha_2, 1-\alpha_1, 1 \\ m_1, m_2, 0 \end{matrix} \right). \quad (15)$$

3. Markov-Chain based Statistical Analysis

Based on the mode of operation, the proposed selection policy, a 2-state ergodic and regular Markov chain is defined, whose state 1 corresponds to the event that FSO link is selected and state 2 corresponds to the event that RF link is selected (see Figure 1). This Markov chain is characterized by a unique vector of stationary probabilities $\pi = [\pi_1, \pi_2]$. Given the fact that the previously mentioned events are mutually exclusive, the CDF of the output SNR at the G using the proposed scheme, γ_t , can be expressed as [27]

$$F_{\gamma_t}(\gamma) = \begin{cases} \sum_{i=1}^2 \pi_i \{ \Pr[\gamma_{th} \leq \gamma_i \leq \gamma] + \Pr[\gamma_i < \gamma_{th}] \\ \quad \times \Pr[\gamma_2 \leq \gamma] \}, & \gamma \geq \gamma_{th} \\ \Pr[\max\{\gamma_1, \gamma_2\} \leq \gamma], & \gamma < \gamma_{th}. \end{cases} \quad (16)$$

where γ_i , with $i \in \{1, 2\}$ denotes the instantaneous received SNR from link i . Based on the definition of the CDF presented in (16) can be expressed as

$$F_{\gamma_t}(\gamma) = \begin{cases} \sum_{i=1}^2 \pi_i \{ F_{\gamma_i}(\gamma) - F_{\gamma_i}(\gamma_{th}) \\ \quad + F_{\gamma_i}(\gamma_{th}) F_{\gamma_i}(\gamma) \}, & \gamma \geq \gamma_{th} \\ F_{\gamma_1}(\gamma) F_{\gamma_2}(\gamma), & \gamma < \gamma_{th} \end{cases} \quad (17)$$

where $F_{\gamma_1}(\cdot), F_{\gamma_2}(\cdot)$ are given by (5) and (15), respectively. Moreover, by differentiating (17) with respect to γ , the following expression for the PDF of γ_t can be obtained

$$f_{\gamma_t}(\gamma) = \begin{cases} \sum_{i=1}^2 \pi_i \{ f_{\gamma_i}(\gamma) + F_{\gamma_i}(\gamma_{th}) f_{\gamma_i}(\gamma) \}, & \gamma \geq \gamma_{th} \\ \sum_{i=1}^2 f_{\gamma_i}(\gamma) F_{\gamma_i}(\gamma), & \gamma < \gamma_{th}, \end{cases} \quad (18)$$

where $f_{\gamma_1}(\cdot), f_{\gamma_2}(\cdot)$ are given by (7) and (14), respectively.

The aforementioned stationary probabilities can be evaluated using $\pi = \pi \cdot \mathbf{P}$ in conjunction with $\sum_{i=1}^2 \pi = 1$, where \mathbf{P} denotes the transition matrix given by

$$\mathbf{P} = \begin{pmatrix} P_{11} & P_{12} \\ P_{21} & P_{22} \end{pmatrix} \quad (19)$$

Exploiting (19), the stationarity probabilities can be obtained as follows

$$\begin{aligned}\pi_1 &= \frac{P_{21}}{P_{12} + P_{21}} \\ \pi_2 &= \frac{P_{12}}{P_{12} + P_{21}}\end{aligned}\quad (20)$$

In (19), the transition probabilities of the corresponding Markov chain can be evaluated using the following formulas

$$P_{i,j} = \begin{cases} \Pr[\gamma_i \geq \gamma_{th}] + \Pr[\gamma_i < \gamma_{th}, \gamma_i \geq \gamma_j], & i = j \\ \Pr[\gamma_i < \gamma_{th}, \gamma_j \geq \gamma_i], & i \neq j. \end{cases} \quad (21)$$

In (21), it is obvious that

$$\Pr[\gamma_i \geq \gamma_{th}] = 1 - F_{\gamma_i}(\gamma_{th}). \quad (22)$$

Moreover,

$$\begin{aligned}\Pr[\gamma_i < \gamma_{th}, \gamma_i \geq \gamma_j] &= \int_0^{\gamma_{th}} \int_0^x f_{\gamma_j}(y) f_{\gamma_i}(x) dy dx \\ &= \int_0^{\gamma_{th}} F_{\gamma_j}(x) f_{\gamma_i}(x) dx.\end{aligned}\quad (23)$$

Furthermore, when $i \neq j$, $P_{i,j} = 1 - P_{i,i}$. All these transition probabilities can be efficiently evaluated by substituting the corresponding PDF and CDF expressions in (22), (23) and employing the Gauss–Laguerre quadrature method [28].

4. Performance Analysis

In this section, analytical expressions for the performance of the scheme under consideration will be provided. More specifically, its performance will be evaluated using the criteria of OP, average NLE and SP.

4.1. Outage Probability

The OP is defined as the probability that the end-to-end instantaneous SNR falls below a predefined threshold γ_T and is given by

$$P_{out} = \Pr[\gamma_o < \gamma_T] = F_{\gamma_o}(\gamma_T). \quad (24)$$

Since a DF relay protocol has been assumed, the CDF of the received SNR γ_o can be expressed as

$$F_{\gamma_o}(\gamma_T) = F_{\gamma_1}(\gamma_T) + F_{\gamma_t}(\gamma_T) - F_{\gamma_1}(\gamma_T)F_{\gamma_t}(\gamma_T), \quad (25)$$

where $F_{\gamma_1}(\gamma_T)$ is given by (5) and $F_{\gamma_t}(\gamma_T)$ is given by (17).

4.1.1. High SNR Analysis

In the high SNR regime, i.e., $\bar{\gamma}_1, \bar{\gamma}_2 \rightarrow \infty$ simpler expressions for (5) and (15) can be obtained. More specifically, using [29, 07.34.06.0006.01] in (5) and after some mathematical simplifications, the following asymptotic closed-form expression is obtained for the CDF of γ_1

$$F_{\gamma_1}(\gamma) \approx \sum_{k=1}^{3b} \frac{\mathcal{A}_i \prod_{\substack{j=1 \\ j \neq k}}^{3b} \Gamma(\mathcal{B}_j - \mathcal{B}_k) \Gamma(1 - \mathcal{D}_1 + \mathcal{B}_k)}{\prod_{j=2}^{b+1} \Gamma(\mathcal{D}_j - \mathcal{B}_k) \Gamma(1 - \mathcal{B}_{3b+1} + \mathcal{B}_k)} \left(\frac{D_i^b \gamma}{b^{2b} \bar{\gamma}_i^f} \right)^{\mathcal{B}_k}, \quad (26)$$

where $\mathcal{D}_1 = 1, \mathcal{D}_2 = \Delta_{b, \zeta_i^2+1}, \mathcal{B}_1 = \Delta_{b, \zeta_i^2}, \mathcal{B}_2 = \Delta_{b, \alpha_i}, \mathcal{B}_3 = \Delta_{b, \beta_i}, \mathcal{B}_4 = 0$. From the above expression, it becomes evident that the diversity gain (G_d) for FSO links, given by $(\bar{\gamma}_i^f)^{-G_d}$ as $\bar{\gamma}_i^f \rightarrow \infty$, depends on the small and large scale turbulence parameters as well as the pointing error coefficient.

As far as the RF link is concerned, by following the same procedure for (15), the corresponding expression is given by

$$F_{\gamma_2}(\gamma) \approx \mathcal{S}_1 \sum_{i=1}^2 \frac{\Gamma(m_{3-i} - m_i) \Gamma(m_i + \alpha_2) \Gamma(m_i + \alpha_1) \Gamma(m_i)}{\Gamma(m_i + 1)} \left(\frac{m_1 m_2 \gamma}{\bar{\gamma}_2} \right)^{m_i}. \quad (27)$$

Following the same approach used for the FSO link, it can be shown that diversity gain for the RF link depends only on the small scale fading parameters.

4.2. Overhead Estimation

In order to quantify the overhead signaling required for the operation of the scheme under consideration two metrics will be adopted, namely the average NLE and the SP.

4.2.1. Average Link Estimation

The overhead and signaling required for allowing the proposed scheme properly function are linear related to the average NLE, which can be evaluated as

$$N = \pi_1(1 + F_{\gamma_1}(\gamma_{th})) + \pi_2(1 + F_{\gamma_2}(\gamma_{th})). \quad (28)$$

From the above equation it can be concluded that the NLEs increases as γ_{th} increases until it reaches to its maximum value that is 2, i.e., always both links are examined before selecting the one that offers the maximum SNR

4.2.2. Switching Probability

Switching between the two links results to increased signalling and also consumes more power. Therefore, SP is one more metric that is related to the overhead signaling of the proposed scheme and is given by

$$S_p = \pi_1(1 - P_{11}) + \pi_2(1 - P_{22}). \quad (29)$$

5. Numerical Results and Discussion

In this section, based on the previous presented theoretical analysis, numerical evaluated results are presented and discussed. If not otherwise stated the values of the parameters considered in these results can be found in Table 1 and are mainly based on previous relevant studies, e.g., [17]. Moreover, for comparison purposes, we have also investigate the performance of a scheme in which the link with the highest SNR, between the RF and the FSO, is always selected. This selection policy is also adopted in [15].

Table 1. Communications Parameters Definitions and Simulation Values

Parameter	Definition	Value
λ_f	FSO wavelength	1550nm
h_s	Satellite height	620km
h_h	HAPS height	20km
h_p	Ground station height	10m
G_{Tf}	Transmit telescope gain	5dB
P_f	FSO transmit power	5dBm
G_{Rf}	Receive telescope gain	10dB
σ_f^2	Variance of the AWGN noise	$4.435 \cdot 10^{-28}$
η	Optical to electrical conversion coefficient	0.8
ζ_i	Pointing error coefficient	13.07
θ	Zenith angle	65°
w	Wind velocity	41m/sec
W_0	Beam radius at the transmitter	2cm
F_0	Phase front radius of curvature of the beam	∞
m_1, m_2	Small scale fading shaping parameters	2.5, 2.8
α_1, α_2	Shadowing shaping parameters	1.2, 1.4
v	Path loss factor	2.1
P_t	Transmit power for RF communications	20dBm
N_0	Noise power	-97.8dBm
G_{T_r}	RF transmit antenna gain	20dB
G_{R_r}	RF receive antenna gain	20dBm
λ_r	RF links wavelength	0.158m

In Figure 2, the performance of both schemes, i.e., the one introduced in this paper, labeled as “Proposed Scheme”, and the one that always selects the highest SNR, labeled as “Maximum SNR”, is evaluated using the criteria of OP (using (25)), the NLE (using (28)), and the SP (using (29)). The performance of these criteria is evaluated as a function of switching threshold γ_{th} , assuming that $\frac{\gamma_T}{\gamma_k} = -10\text{dB}$. It is shown that as γ_{th} increases, the OP performance of the proposed scheme approaches the one of Maximum SNR. What is very important to be noted is that the proposed scheme offers a considerable improvement on overhead estimation criteria that have been examined in this paper, namely the NLE and PS. For example, for $\gamma_{th} = 5\text{dB}$, the OP is equal for both schemes, while SP is 10 – 14% lower for the proposed scheme, while the NLE is more than 70% lower. Therefore, based on the results of this figure, it can be concluded that in the proposed scheme, an excellent compromise between performance improvement and overhead reduction can be achieved by setting $\gamma_{th} = \gamma_T$.

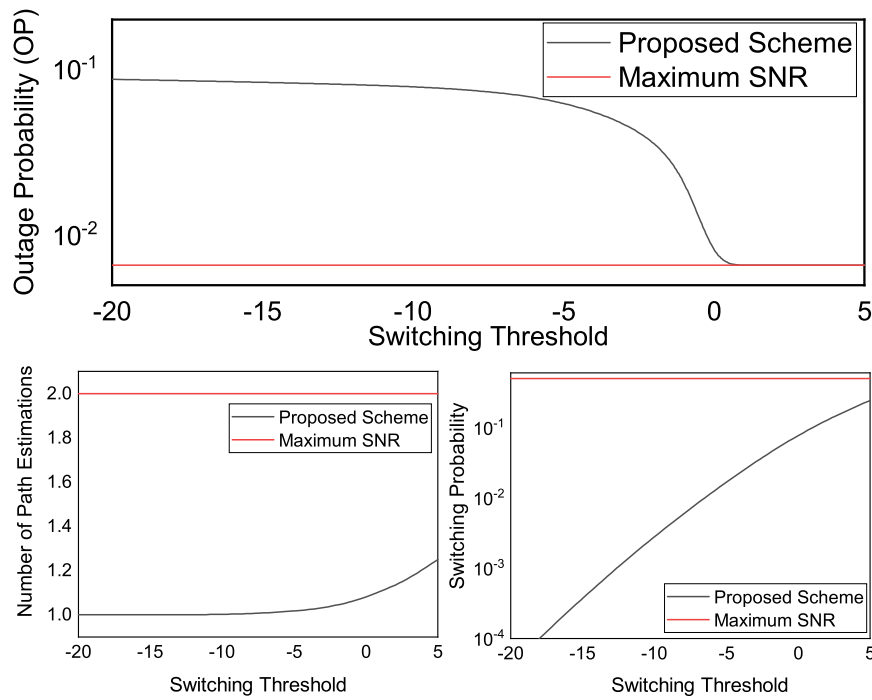


Figure 2. OP vs average SNR for various propagation conditions.

In Figure 3, an effort to depict the impact of the wind velocity w to the OP has been made. More specifically, the OP is plotted as a function of the average SNR (assuming $\tilde{\gamma}_1 = \tilde{\gamma}_2$). In this figure, it is shown that the OP improves as the wind velocity increases, with the highest improvement being noticed when w decreases from 51m/s to 31m/s. In the same figure and using the corresponding high SNR expression for the CDF, based on (26) and (27), it is proved the excellent tightness between the exact and the asymptotic results. In Figure 4, the impact of the elevation angle θ on the OP of the proposed scheme has been evaluated. More specifically, the OP is plotted as a function of the average SNR for various values of θ . It is shown that the performance improves as θ decreases. Moreover, an excellent tightness is also observed between the exact and the asymptotic results.

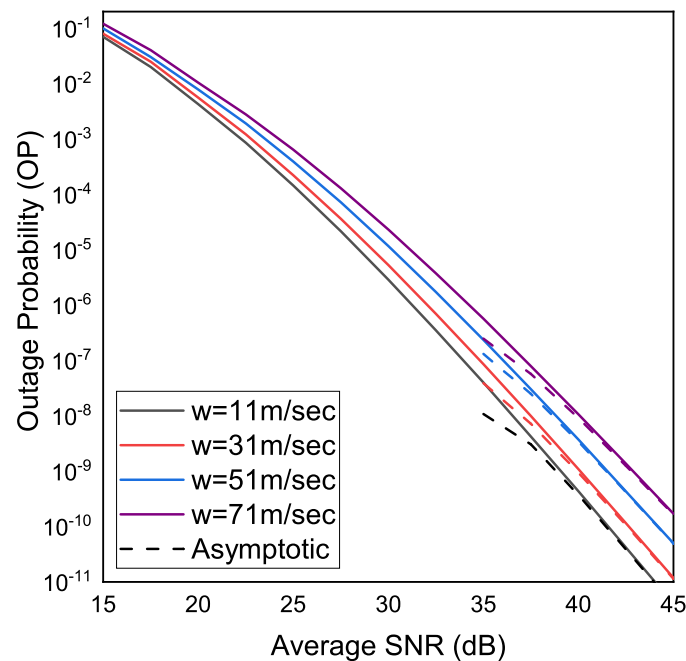


Figure 3. OP vs average SNR for various propagation conditions.

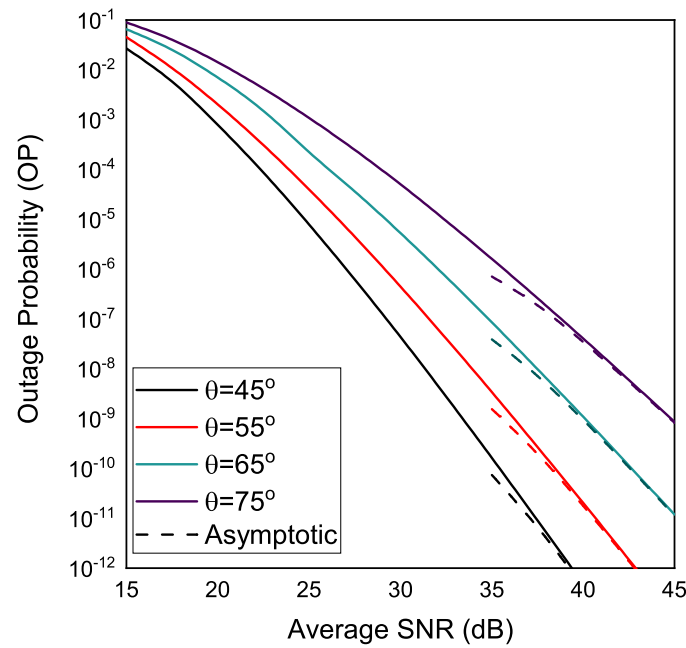


Figure 4. OP vs average SNR for various propagation conditions.

Finally, in Figure 5, the impact of small and large scale fading, which are controlled by parameters m, α , respectively, on the OP and SP has been evaluated. In these figures it is shown the important difference that exist between the two limiting scenarios, i.e., the one with light fading/shadowing conditions ($m = 3, \alpha = 1$) and the one with severe fading/shadowing ($m = 1, \alpha = 3$). For the other scenarios under investigation, it seems that when light fading and severe shadowing exists, i.e., $m = 3, \alpha = 1$, the performance is better for lower values of the average SNR, as compared to the reverse scenario. As far as the SP is concerned, it is depicted that for all scenarios investigated, except the one with good fading/shadowing conditions, as the average SNR increases the performances become equal.

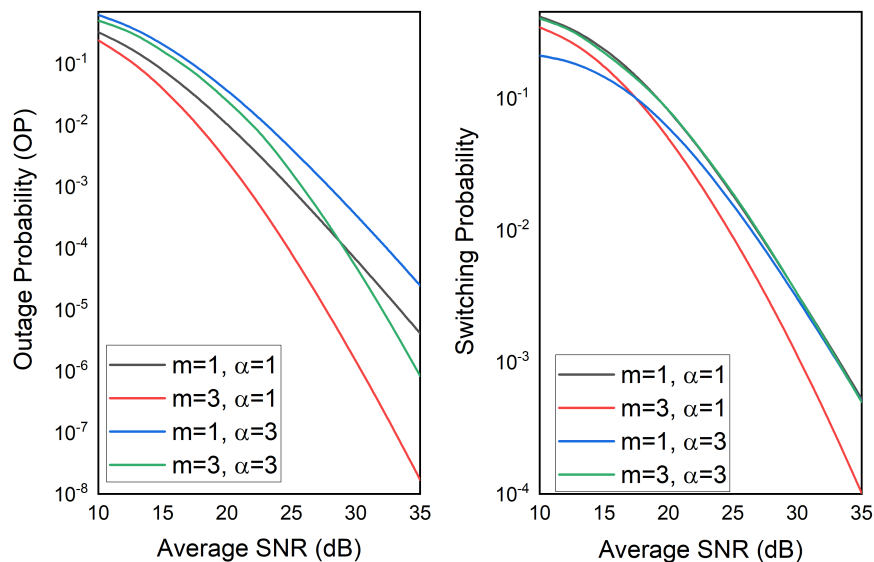


Figure 5. OP vs average SNR for various propagation conditions.

6. Conclusions

In this paper, a new channel selection policy is employed in hybrid FSO/RF SAGIN. This policy can dynamically improve the system's performance or reduce the overhead signalling according to the

network operator requirement. To this aim, a stochastic analysis has been performed to investigate the end-to-end outage probability. Moreover, the overhead has been evaluated using the criteria of switching probability and average number of link selection. It has been shown that the proposed scheme offers similar OP performance with an other benchmark with reduced however overhead. As a future step, it is planned to investigate the impact of time correlated fading to the proposed system's performance.

Author Contributions: Conceptualization, P.S.B. and H.E.N.; methodology, P.S.B.; software, P.S.B.; validation, P.S.B., H.E.N., A.K. and L.Y.; writing—original draft preparation, P.S.B.; writing—review and editing, P.S.B., H.E.N., A.K. and L.Y.; visualization, P.S.B.; supervision, H.E.N. All authors have read and agreed to the published version of the manuscript.

Conflicts of Interest: The authors declare no conflict of interest.

Abbreviations

The following abbreviations are used in this manuscript:

AWGN	Additive White Gaussian Noise
CDF	Cumulative Distribution Function
DF	Decode-and-Forward
FSO	Free Space Optical
HAPS	High Altitude Platform Station
LEO	Low Earth Orbit
NLE	Number of Link Estimation
OP	Outage Probability
PDF	Probability Density Function
RF	Radio Frequency
RIS	Reconfigurable Intelligent Surface
SAGIN	Satellite Aerial Ground Integrated Networks
SNR	Signal to Noise Ratio
SP	Switching Probability
UAV	Unmanned Aerial Vehicles

References

1. Liu, J.; Shi, Y.; Fadlullah, Z.M.; Kato, N. Space-air-ground integrated network: A survey. *IEEE Communications Surveys & Tutorials* **2018**, *20*, 2714–2741. doi:10.1109/COMST.2018.2841996.
2. Guo, H.; Li, J.; Liu, J.; Tian, N.; Kato, N. A survey on space-air-ground-sea integrated network security in 6G. *IEEE Communications Surveys & Tutorials* **2022**, *24*, 53–87. doi:10.1109/COMST.2021.3131332.
3. Shang, B.; Yi, Y.; Liu, L. Computing over space-air-ground integrated networks: challenges and opportunities. *IEEE Network* **2021**, *35*, 302–309. doi:10.1109/MNET.011.2000567.
4. Ye, J.; Dang, S.; Shihada, B.; Alouini, M.S. Space-air-ground integrated networks: Outage performance analysis. *IEEE Transactions on Wireless Communications* **2020**, *19*, 7897–7912. Cited by: 66; All Open Access, Green Open Access, doi:10.1109/TWC.2020.3017170.
5. Niu, Z.; Shen, X.S.; Zhang, Q.; Tang, Y. Space-air-ground integrated vehicular network for connected and automated vehicles: Challenges and solutions. *Intelligent and Converged Networks* **2020**, *1*, 142–169.
6. Anandkumar, D.; Sangeetha, R. A survey on performance enhancement in free space optical communication system through channel models and modulation techniques. *Optical and Quantum Electronics* **2021**, *53*, 1–39.
7. Nadeem, F.; Kvicera, V.; Awan, M.S.; Leitgeb, E.; Muhammad, S.S.; Kandus, G. Weather effects on hybrid FSO/RF communication link. *IEEE Journal on Selected Areas in Communications* **2009**, *27*, 1687–1697. doi:10.1109/JSAC.2009.091218.
8. Barrios, R.; Dios, F. Exponentiated Weibull distribution family under aperture averaging for Gaussian beam waves. *Optics express* **2012**, *20*, 13055–13064.

9. Usman, M.; Yang, H.C.; Alouini, M.S. Practical switching-based hybrid FSO/RF transmission and its performance analysis. *IEEE Photonics journal* **2014**, *6*, 1–13.
10. Kurt, G.K.; Khoshkholgh, M.G.; Alfattani, S.; Ibrahim, A.; Darwish, T.S.; Alam, M.S.; Yanikomeroglu, H.; Yongacoglu, A. A vision and framework for the high altitude platform station (HAPS) networks of the future. *IEEE Communications Surveys & Tutorials* **2021**, *23*, 729–779.
11. Jia, Z.; Sheng, M.; Li, J.; Han, Z. Toward data collection and transmission in 6G space–air–ground integrated networks: Cooperative HAP and LEO satellite schemes. *IEEE Internet of Things Journal* **2021**, *9*, 10516–10528.
12. Liu, X.; Lin, M.; Zhu, W.P.; Wang, J.Y.; Upadhyay, P.K. Outage performance for mixed FSO-RF transmission in satellite-aerial-terrestrial networks. *IEEE Photon. Technol. Lett.* **2020**, *32*, 1349–1352. doi:10.1109/LPT.2020.3025452.
13. Kong, H.; Lin, M.; Zhu, W.P.; Amindavar, H.; Alouini, M.S. Multiuser Scheduling for Asymmetric FSO/RF Links in Satellite-UAV-Terrestrial Networks. *IEEE Wireless Communications Letters* **2020**, *9*, 1235 – 1239. Cited by: 72, doi:10.1109/LWC.2020.2986750.
14. Swaminathan, R.; Sharma, S.; Vishwakarma, N.; Madhukumar, A. HAPS-based relaying for integrated space–air–ground networks with hybrid FSO/RF communication: A performance analysis. *IEEE Trans. Aerosp. Electron.* **2021**, *57*, 1581–1599.
15. Yahia, O.B.; Erdogan, E.; Kurt, G.K.; Altunbas, I.; Yanikomeroglu, H. HAPS selection for hybrid RF/FSO satellite networks. *IEEE Trans. Aerosp. Electron.* **2022**, *58*, 2855–2867.
16. Yahia, O.B.; Erdogan, E.; Kurt, G.K. HAPS-assisted hybrid RF-FSO multicast communications: Error and outage analysis. *IEEE Trans. Aerosp. Electron.* **2023**, *59*, 140–152. doi:10.1109/TAES.2022.3186296.
17. Samy, R.; Yang, H.C.; Rakia, T.; Alouini, M.S. Hybrid SAG-FSO/SH-FSO/RF transmission for next-generation satellite communication systems. *IEEE Transactions on Vehicular Technology* **2023**, pp. 1–13. doi:10.1109/TVT.2023.3281256.
18. Li, X.; Li, Y.; Song, X.; Shao, L.; Li, H. RIS assisted UAV for weather-dependent satellite terrestrial integrated network with hybrid FSO/RF systems. *IEEE Photonics Journal* **2023**.
19. Michailidis, E.T.; Bithas, P.S.; Nomikos, N.; Vouyioukas, D.; Kanatas, A.G. Outage probability analysis in multi-user FSO/RF and UAV-enabled MIMO communication networks. *Physical Communication* **2021**, *49*, 101475. doi:https://doi.org/10.1016/j.phycom.2021.101475.
20. Sharif, S.; Zeadally, S.; Ejaz, W. Space-aerial-ground-sea integrated networks: Resource optimization and challenges in 6G. *Journal of Network and Computer Applications* **2023**, *215*, 103647. doi:https://doi.org/10.1016/j.jnca.2023.103647.
21. Viswanath, A.; Jain, V.K.; Kar, S. Analysis of earth-to-satellite free-space optical link performance in the presence of turbulence, beam-wander induced pointing error and weather conditions for different intensity modulation schemes. *IET Communications* **2015**, *9*, 2253–2258.
22. Sharma, S.; Madhukumar, A.; Ramabadran, S. Performance of dual-hop hybrid FSO/RF system with pointing errors optimization. *IEEE 91st Vehicular Technology Conference*, 2020, pp. 1–5.
23. Kaushal, H.; Kaddoum, G. Optical communication in space: Challenges and mitigation techniques. *IEEE Commun. Surv. Tutor.* **2016**, *19*, 57–96.
24. Gradshteyn, I.S.; Ryzhik, I.M. *Table of Integrals, Series, and Products*, 6 ed.; Academic Press: New York, 2000.
25. Viswanath, A.; Gopal, P.; Jain, V.K.; Kar, S. Performance enhancement by aperture averaging in terrestrial and satellite free space optical links. *IET Optoelectronics* **2016**, *10*, 111–117.
26. Bithas, P.S.; Nikolaidis, V.; Kanatas, A.G.; Karagiannidis, G.K. UAV-to-Ground communications: Channel modeling and UAV selection **2020**. *68*, 5135–5144.
27. Bithas, P.S.; Rontogiannis, A.A.; Karagiannidis, G.K. An Improved Threshold-Based Channel Selection Scheme for Wireless Communication Systems **2016**. *15*, 1531–1546.
28. Abramowitz, M.; Stegun, I.A. *Handbook of mathematical functions: with formulas, graphs, and mathematical tables*; Vol. 55, Courier Corporation, 1964.
29. The Wolfram Functions Site., 2023.

Disclaimer/Publisher’s Note: The statements, opinions and data contained in all publications are solely those of the individual author(s) and contributor(s) and not of MDPI and/or the editor(s). MDPI and/or the editor(s) disclaim responsibility for any injury to people or property resulting from any ideas, methods, instructions or products referred to in the content.